Chapter III. Engineering complex phenotypes by reprogramming alternative splicing

Abstract

Alternative splicing affects more than 90% of human genes, increases proteomic diversity, controls gene expression and contributes significantly to the high level of phenotypic complexity in mammals[1]. The ability to program alternative splicing patterns will provide a powerful tool to interrogate and manipulate cellular function. Toward this aim, we have developed a novel framework for the construction of single input-single output RNA control devices based on the direct coupling of a sensor component, composed of a protein-binding RNA aptamer and an actuator component, composed of an alternatively spliced transcript. These devices function to sense changes in intracellular protein concentrations to regulate alternative splicing and the expression of any gene. This framework can be extended to process multiple inputs and to rewire endogenous signal transduction pathways to create novel regulatory networks for user defined phenotypes. Our devices can therefore integrate cellular information by linking external stimuli to complex phenotypes, thus controlling cellular function. This platform provides a novel class of RNA-based "smart" therapeutics towards the treatment and diagnosis of disease.

3.1. Introduction

Normal cellular functions depend on the tight regulation of post-transcriptional gene regulatory mechanisms. One such process is alternative splicing, which produces multiple protein isoforms from a single gene by altering the ways in which exons are joined from a single pre-mRNA[2]. The regulation of alternative splicing is critical for the temporal and spatial expression of cellular factors[3]. Splicing patterns are tightly regulated by the interplay between auxiliary *cis*-acting elements and the trans-acting factors that modulate them, leading to a 'splicing code' that is susceptible to mutations and misregulation[4]. Up to 50% of disease-causing mutations affect splicing yielding a variety of therapeutic targets, shedding light on the need for the development of tools that reprogram splicing decisions[3]. Recently, synthetic RNA-based regulatory systems that process small molecule inputs have been developed towards the regulation of pre-mRNA splicing in yeast and mammalian cells [5]. The extension of these designs as cellular therapeutics has been hampered by the limited number of aptamer domains that can be used in the engineering of these platforms and the utility of existing ligands which are restricted by the lack of cell permeability and toxicity to cells [5]. Moreover, there are only a few examples of synthetic and naturally occurring protein-dependent RNA-based regulatory systems [6–8]. Since much of cellular physiology is regulated by protein expression and activity, the ability to interrogate and regulate these processes is an important goal in biological and medical research. Given the unique properties of synthetic RNA-based regulatory systems that are suitable for therapeutic applications, including tunable regulation and rapid response times to input availability[8], the creation of such a system towards the regulation of alternative splicing based on sensing protein biomarkers would have broad applications in biotechnology and medicine.

3.2. Results

Here, we describe a novel framework for the construction of single input-single output RNA control devices based on the direct coupling of a sensor component, composed of a protein-binding RNA aptamer and an actuator component, composed of an alternatively spliced transcript. This framework consists of a reporter construct that expresses the gene encoding the green fluorescent protein (GFP) fused 3'of a three exon, two-intron mini-gene. The alternatively-spliced transcript contains a middle exon that harbors a stop codon and a protein binding aptamer positioned in either of two introns (Figure 3.1a). Regulation of this device is exerted by RNA aptamers that sense intracellular changes in protein concentration and alter splice site selection through steric hindrance of spliceosomal components either at the 3'or 5' splice sites (ss). Therefore, cells with a high level of exon inclusion should display lower GFP fluorescence than cells in which this exon is excluded.

We implemented the platform with the SMN1 mini-gene as an actuator and the MS2 coat protein binding aptamer as the sensor component[9,10]. To determine the utility of this device, we preformed a systematic experimental analysis of aptamer mediated regulation of splicing by inserting the MS2 coat protein aptamer at various positions upstream the 3'ss and downstream the 5'ss (Figure 3.1b). Starting at both consensus splice sites the MS2 aptamer was inserted into 6 separate positions spaced by 15-nucleotides (nts). The resulting constructs were stably integrated into HEK-293 FLP-In cells to generate isogenic cell lines. To assess the effect of the MS2 coat protein on reporter gene splicing, we transiently expressed an MS2 coat protein fusion with monomeric DsRed and an SV40 NLS in these stable cell lines (Figure 3.1b). The nuclear

localization of the MS2-DsRed fusion was confirmed by confocal microscopy (data not shown). In the presence of the MS2-DsRed fusion we find that 3 positions exhibit significant silencer activity ($P < 0.05$) near both splice sites, while 2 near the 3'ss and 1 near the 5'ss exhibit enhancer activity as compared to the expression of DsRed alone ($P < 0.05$) (Figure 3.1c). These results demonstrate that aptamer-regulated control is position dependent and likely occurs through steric hindrance of spliceosome assembly.

To examine changes in splicing patterns, we analyzed the transcript isoforms of the devices and controls in the presence and absence of the MS2-DsRed fusion by qRT-PCR. The exon exclusion to inclusion ratios for each device (Figure 3.1d) significantly correlates with the observed relative device expression in Figure 3.1c ($P << 0.01$, ANOVA). To examine the regulatory effect of the insertion of the MS2 aptamer into the SMN1 transcript we compared the fluorescence of our devices to the wildtype mini-gene in the absence of the MS2-DsRed fusion. The aptamer secondary structure alone has a significant effect on the regulation of the SMN1 transcript, where the majority of positions display significant silencer activity (Figure 3.1e). Interestingly, the effect of RNA secondary structure was insignificant at position 3 (MS2-3) which displayed significant silencer activity in our expression studies; whereas the presence of the MS2 aptamer at position 10 (MS2-10) had the opposite effect of what was observed in the expression studies. Therefore, the modulation of RNA secondary structure within introns of alternatively spliced transcripts may be a component of future design efforts for these frameworks. The exon exclusion to inclusion expression ratios confirm the regulatory activity of our synthetic devices observed by fluorescence measurements and that secondary structure alone can modulate splicing patterns.

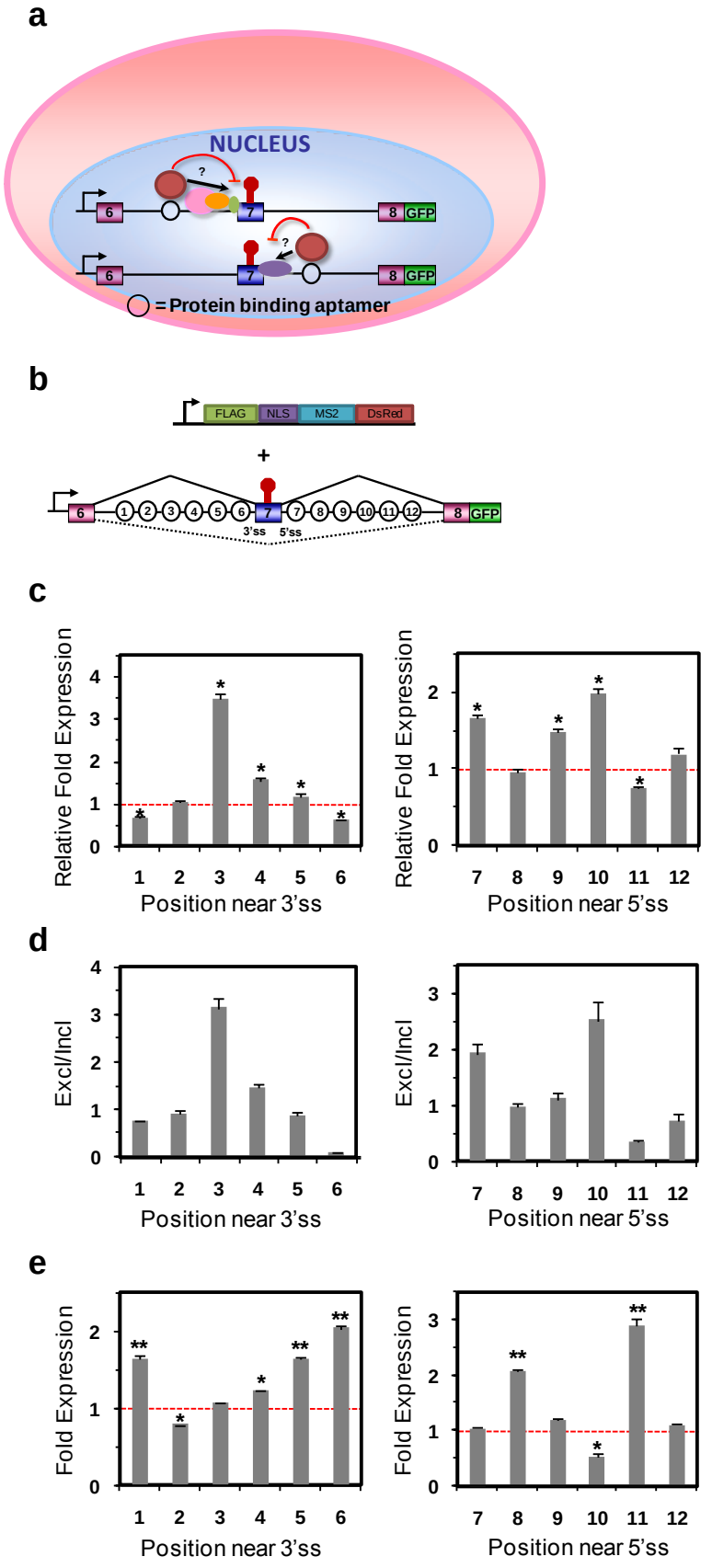
a
NUCLEUS
6
7
8 GFP
= Protein binding aptamer
b
FLAG
NLS
MS2
DsRed
+
3'ss
5'ss
c
Relative Fold Expression
Position near 3'ss
Position near 5'ss
d
Excl/Incl
Position near 3'ss
Position near 5'ss
e
Fold Expression
Position near 3'ss
Position near 5'ss

Figure 3.1. RNA device framework and analysis. **(a)** Aptamer-based splicing regulatory platform. The framework consists of a fluorescent reporter protein (GFP) fused 3' of the SMN1 mini-gene. The SMN1 mini-gene contains an alternative exon (exon 7) that harbors a stop codon and a protein binding aptamer in either of two introns. **(b)** Platform used for the systematic analysis of aptamer mediated regulation of alternative splicing and heterologous MS2-DsRed fusion construct. Starting at both consensus splice sites, the MS2 aptamer was inserted into 6 separate positions (1-6 near 3'ss and 7-12 near 5'ss) spaced by 15-nucleotides. The FLAG-NLS-MS2-DsRed fusion construct was expressed in the HEK-293 stable cell lines contacting these devices. **(c)** Flow cytometry analysis of HEK-293 FLP-In stable cell lines containing the MS2 regulatory devices. For all reported activities, the mean GFP levels from two independent experiments were determined and normalized to the mutant devices in the presence and absence of ligand. Relative fold expression and average error are reported. *P*-values derived from the Student's t-test are as follows: $*P < 0.05$ and $**P < 0.01$. **(d)** qRT-PCR analysis of the MS2 regulatory devices with primer sets specific for exon 7 included and excluded products. Expression levels of duplicate PCR samples were normalized to the levels of *HPRT*. Data is reported as the ratio of the mean expression of the exon excluded isoform to the exon included isoform normalized to the ratio for the mutant control device ± the average error. **(e)** Flow cytometry analysis of HEK-293 FLP-In stable cell lines containing the MS2 regulatory devices normalized to the wild-type SMN1 mini-gene in the absence of the MS2-DsRed fusion.

To demonstrate the functional modularity of our platform and to investigate the ability to rationally reprogram natural signal transduction pathways using our devices, we replaced the MS2 sensor component with RNA aptamers towards β-catenin, NF-κB p50 and NF-κB p65. Initially to examine the modularity of our device we replaced the MS2 aptamer with an RNA aptamer towards β-catenin as well as mutant aptamer that is the reverse compliment of the β-catenin aptamer at the positions exhibited the most significant suppression and enhancement of splicing by MS2; 3 and 6 within our framework (Figure 3.1b)[11]. β-catenin is a central component of the well-characterized Wnt pathway that regulates cell growth and differentiation during embryonic development and tumorigenesis [11]and during tumorigenesis β-catenin is nuclear localized to regulate the transcription of oncogenic target genes [11]. The β-catenin devices were stably integrated into HEK-293 FLP-In cells and leukotriene D_4 (LTD_4) was added to induce β-catenin signaling and translocation to the nucleus (Figure 3.2a). The regulatory activity of these devices was assessed over a 48 h time period in the presence of LTD_4 compared to control constructs which contain a mutant β-catenin aptamer (B-catΔ) (Figure 3.2b). The B-cat-6 device response demonstrates increasing gene expression over time ($P < 0.05$), corresponding to an increase in exon skipping (Figure 3.2b). These results demonstrate component modularity of our platform and the ability to sense and rewire endogenous signal transductions pathways. In contrast, the B-cat-3 device does not respond to LTD_4 stimulated β-catenin signaling. The MS2 device studies demonstrated exon enhancement at position 6, where as the B-cat-6 device shows increased skipping. As compared to the MS2 studies, the β-catenin device responses suggest that different proteins ligands likely have varying positional effects on splicing as

result of protein-protein interactions, steric hindrance of spliceosome machinery and specific RNA structural modification resulting from ligand binding.

To further examine component modularity and to reprogram additional signaling pathways, we inserted aptamers towards NF-κB p50 and NF-κB p65 into position 3 of our platform (Figure 3.2c). The NF-κB p50 and p65 dimers play a significant role in inflammation and disease by binding to κB sites in promoters or enhancers of target genes[12]. Two aptamers towards NF-κB p50 (p50(1) and p50(2)) and one towards p65 were individually inserted into our platform as were mutant versions of these aptamers [12-14]. These devices were stably integrated into HEK-293 FLP-In cells and tumor necrosis factor alpha (TNF-α) was supplemented to induce NF- κB signaling and subsequent translocation of NF- κB to the nucleus (Figure 3.2c)[15]. The regulatory activity of these devices was assessed over a 48 h time period (Figure 3.2d). The p65-3 device displays increasing gene expression over time ($P < 0.01$), corresponding to an increase in exon skipping (Figure 3.2d). These results further demonstrate the component modularity of our platform and regulatory functionalities in which different ligands can achieve significant suppression of splicing at a single site.

Interestingly, both p50-3 devices show a decrease in gene expression ($P < 0.05$), correlating with a decrease in exon skipping. To determine whether the NF- κB devices response to TNF-α is directly mediated by NF- κB, we developed a p50-DsRed fusion construct (Figure 3.2e). The p50-DsRed fusion construct was transiently expressed in the stable cell lines containing the NF- κB p50 devices and regulatory activity of these devices was assessed in the presence of the fusion and absence of the fusion compared to mutant aptamer containing control constructs (Figure 3.2f). Both device output responses

(p50(1) and p50(2)) demonstrate decreasing gene expression ($P < 0.05$) and correlate well with the observed changes in gene expression seen with TNF-α stimulated NF- κB regulation (Figure 3.2d). Furthermore, these results suggest that our signal transduction device responses are due to specific effector-mediated gene regulatory effects imparted by highly specific target recognition abilities and that different protein binding at a given site will impart differential regulation. As such, aptamer position and the target protein will provide key tuning capabilities for our devices.

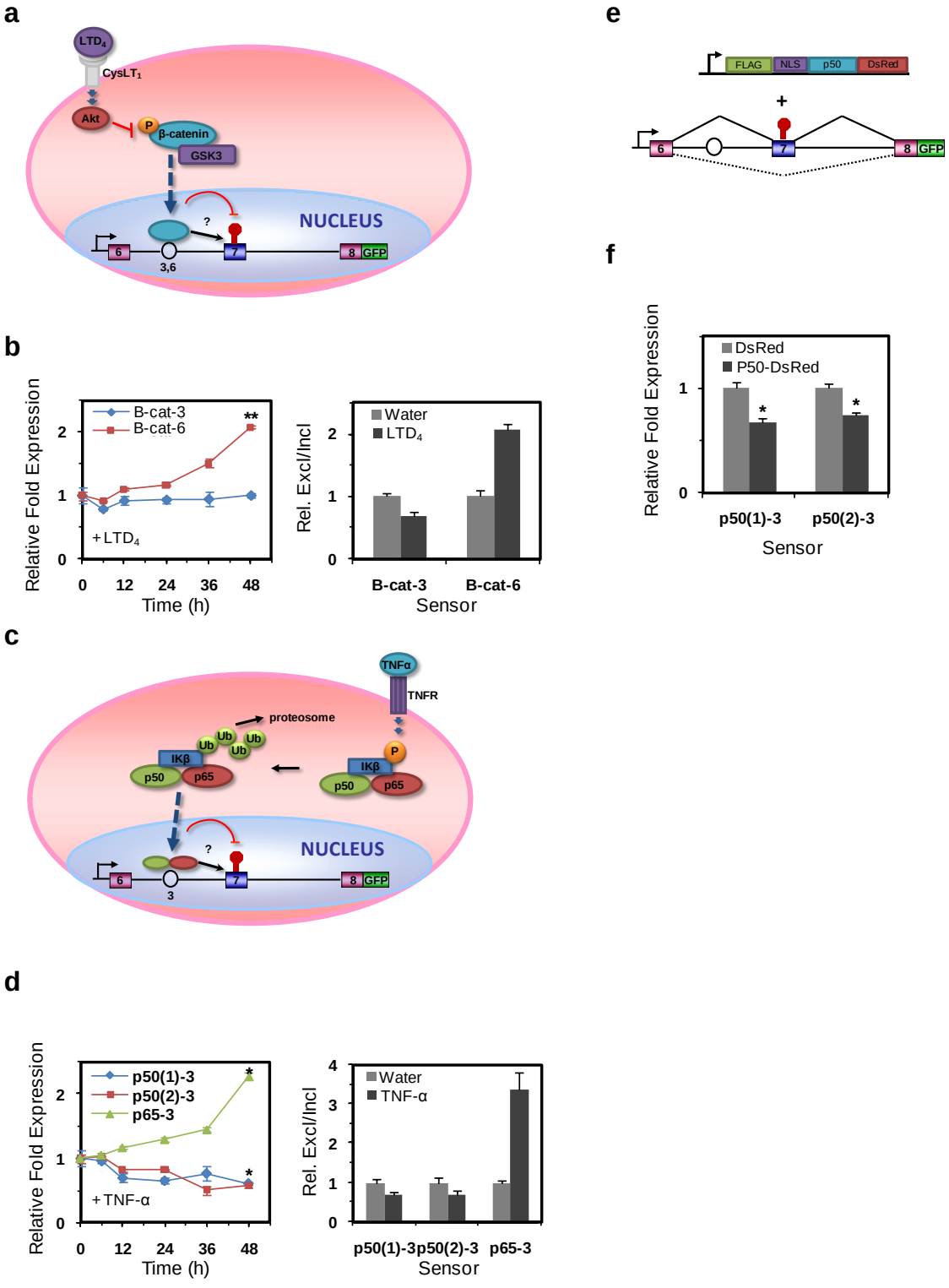

Figure 3.2. RNA device component modularity and reprogramming of endogenous signaling pathways. **(a)** Schematic of the translocation of β-catenin into the nucleus upon

stimulation by LTD_4 where binding of the RNA aptamer alters splice site choice. **(b)** Flow cytometry and qRT-PCR analysis of HEK-293 FLP-In stable cell lines containing the β-catenin regulatory devices (B-cat-3 and B-cat-6). Cells were stimulated with 80 nM LTD_4 for 48 h. **(c)** Schematic of the translocation of NF-κB dimers p50 and p65 into the nucleus upon stimulation by TNF-α where binding of the RNA aptamer alters splice site choice. **(d)** Flow cytometry and qRT-PCR analysis of HEK-293 FLP-In stable cell lines containing the NF-κB regulatory devices (p50(1)-3, p50(2)-3 and p65-3). Cells were stimulated with 20ng/ml TNF-α for 48 h. **(e)** Platform used for the analysis of NF-κB p50 mediated regulation of alternative splicing and heterologous p50-DsRed fusion construct. **(f)** Flow cytometry analysis of HEK-293 FLP-In stable cell lines containing the NF-κB p50 regulatory devices. Regulatory activity was assessed in the presence of the p50-DsRed fusion and absence of the fusion (DsRed only) compared to mutant aptamer containing control constructs.

To enable the design of complex gene circuits, there is a need for modular genetic components that can be used to sense different stimuli and generate stimulus specific phenotypes. To extend our regulatory platform towards multiple input processing we integrated both wildtype and mutant MS2 sensor components into positions 3 and 10 of the framework (Figure 3.3a). These devices were stably integrated into HEK-293 and the output response of the devices was examined in the presence and absence of the MS2-DsRed fusion. The regulatory response of the device is low in the absence of the MS2-DsRed fusion (Figure 3.3b). In contrast, the responses at both positions are equivalent with a significant increase in gene expression ($P < 0.01$). The combination of both inputs

yields a slightly higher response (~.5 fold) than the individual inputs ($P < 0.01$). The exon exclusion to inclusion ratios in the absence the MS2-DsRed fusion are undetectable, while each MS2-DsRed input and in combination show a significant increase in exon exclusion validating the platforms regulatory function (Figure 3.3c).

We adapted our multi-input platform to process both the heterologous MS2-DsRed and the endogenous NF-κB p50 inputs, by replacing the MS2 aptamer in position 3 with the aptamer towards NF-κB p50 (Figure 3.3d). Likewise, mutants of both aptamers were inserted into the framework. These devices were stably integrated into HEK-293 and the output response of the devices was examined in absence of both inputs (p50 and MS2) and in the presence of either input or both (Figure 3.3e). We find that the output response is low in the absence of both ligands. The device response at both positions is equivalent to the regulatory activity observed with our single input devices demonstrating that platform function is programmable (Figures. 3.1c and 3.2d), where the platform response to p50 is that decreased gene expression, where as the response to MS2-DsRed is of increased gene expression ($P < 0.05$). Interestingly, the device response in the presence of both ligands is greater than the sum of the individual components, suggesting the combined inputs have a synergistic or combinatorial effect on splicing regulation. The transcript isoform ratios for the devices correlate well with the observed gene expression responses and therefore validate their regulatory function (Figure 3.3f).

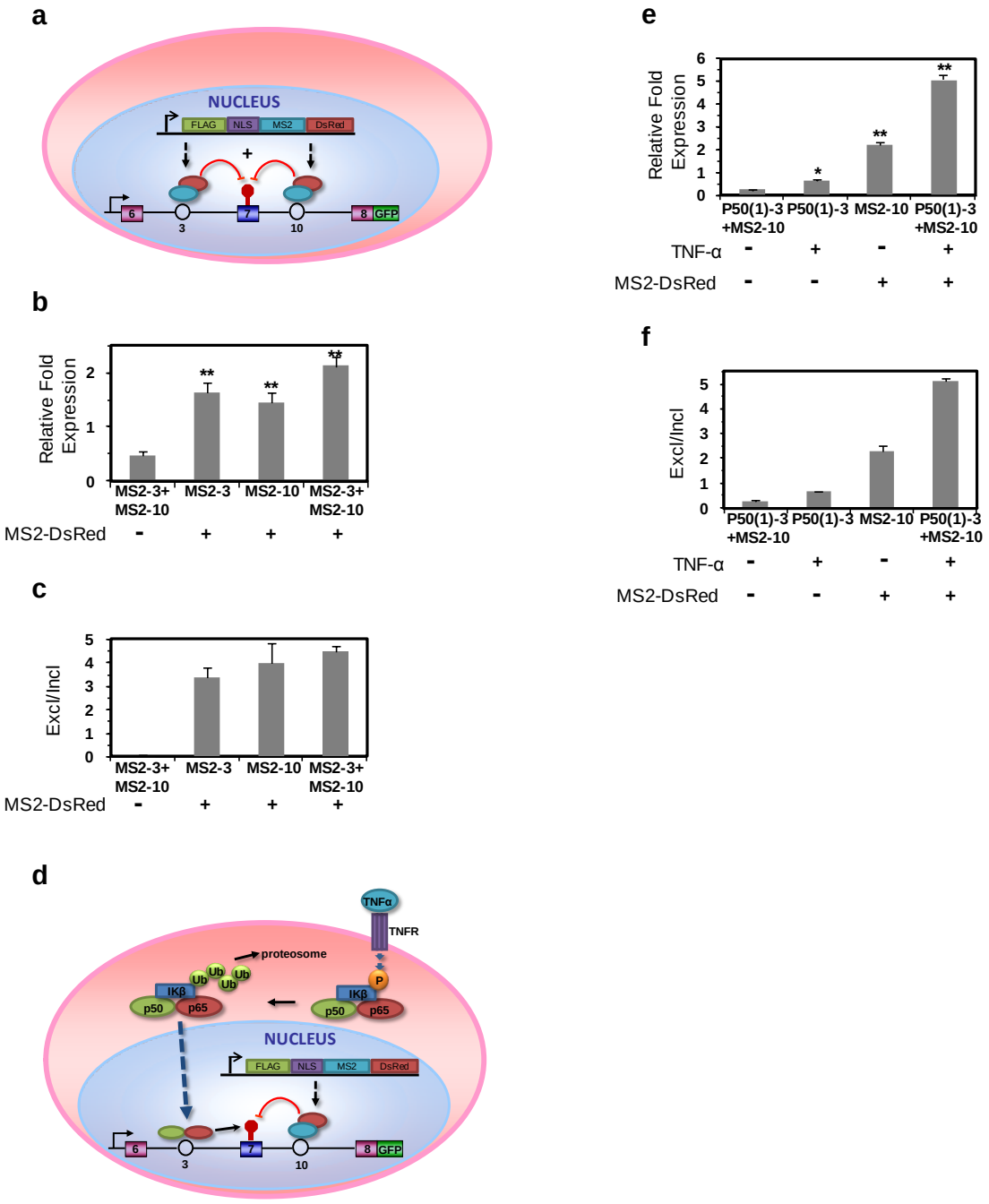

Figure 3.3. Multi-input processing platform and analysis. **(a)** MS2 multi-input splicing regulatory platform. The MS2 sensor components were inserted into positions 3 and 10 of the framework. **(b)** Flow cytometry analysis of HEK-293 FLP-In stable cell lines containing the MS2 multi-input regulatory devices. Regulatory activity was assessed in

the presence of the MS2-DsRed fusion and absence of the fusion (DsRed only) compared to mutant aptamer containing control constructs. **(c)** qRT-PCR analysis of HEK-293 FLP-In stable cell lines containing the MS2 multi-input regulatory devices. **(d)** MS2 and NF-κB p50 multi-input splicing regulatory platform. The NF-κB p50 and MS2 sensor components were inserted into positions 3 and 10 of the framework respectively. Cells were stimulated with 20ng/ml TNF-α to induce the NF-κB pathway and the MS2-DsRed fusion construct was transiently expressed. **(e)** Flow cytometry analysis of HEK-293 FLP-In stable cell lines containing the MS2 and NF-κB p50 multi-input regulatory devices. Regulatory activity was assessed in the absence of the both inputs (MS2-DsRed fusion and TNF- α) and in the presence of either input or both. **(f)** qRT-PCR analysis of HEK-293 FLP-In stable cell lines containing the MS2 and NF-κB p50 multi-input regulatory devices.

To investigate whether our platform can be used to regulate biological processes, we replaced the GFP reporter in our MS2-3 mutant and wildtype devices with *Puma*, a proapoptotic gene (Figure 3.4a). It has been demonstrated that the overexpression of Puma induces rapid apoptosis in mammalian cells through a Bax- and mitochondria-dependent pathway[16]. Apoptosis was assessed by flow cytometry 48h after transfection of the MS2-DsRed fusion. We find that apoptosis was significantly induced in cells containing the wildtype MS2-3 device as compared to cells containing the mutant device MS2Δ-3 which displayed an insignificant change in apoptosis (Figure 3.4b). To examine the ability to rationally reprogram signal transduction pathways to regulate apoptosis, we replaced the MS2 aptamer with the wildtype and mutant aptamers towards β-catenin (position 6) and NF-κB p65 (position 3) (Figure 3.4c). These aptamers were chosen

because they demonstrated increased exon exclusion activities which should upregulate the expression of Puma. LTD_4 or TNF-α was added to HEK-293 stable cell lines containing these devices to induce either the β-catenin or NF-κB pathway. Apoptosis was significantly induced in cells containing the B-cat-6 ($P < 0.01$) and p65-3 devices ($P < 0.05$), while cells containing the mutant devices (B-catΔ-6 and p65Δ-3) did not display a change in apoptosis (Figure 3.4d). The device mediated regulation of Puma and resulting apoptosis is in line with percentages observed in Puma overexpression studies[17]. These results show that both heterologous as well as endogenous inputs can be processed by our platform to regulate apoptosis.

To demonstrate the scalability of our platform in regulating apoptosis, we replaced Puma with the suicide gene therapy system, herpes simplex thymidine kinase (HSV-TK) in devices regulated by β-catenin and NF-κB p65 (Figure 3.4e). The HSV-TK system confers sensitivity to the prodrug ganciclovir (GCV) and has been shown to induce apoptosis in target cells[18]. We examined HSV-TK/GCV-induced apoptosis in HEK-293 cell lines stably expressing these devices in the presence of varying amounts (10 or 100 μM) and in the absence of GCV. To induce either the β-catenin or NF-κB pathway, LTD_4 or TNF-α was added to these cell lines. The B-cat-6 wildtype device in the presence of LTD_4 demonstrates significant sensitivity to GCV with an average cell survival of ~21% at 100 μM GCV ($P < 0.01$) (Figure 3.4f). In contrast, B-catΔ-6 in the presence and B-cat-6 in the absence of LTD_4, displayed similar survival rates of ~60%. The observed reduced cell survival may due to having sufficient expression of the basal spliced HSV-TK isoform to induce apoptosis upon addition of GCV as well as high dosages of GCV alone have been shown to induce cell death in the ranges of 5–30% in

cell culture [19]. In the presence of TNF-α, the wildtype p65-3 device demonstrates significant sensitivity to GCV with an average survival of ~23% at 100 μM GCV ($P < 0.01$), while the p65Δ-3 device shows little sensitivity with average survival of ~93% at 100 μM GCV. Similar to the B-cat-6 devices, the wildtype p65-3 device in the absence of TNF-α shows some sensitivity to GCV with an average survival of ~70% at 100 μM GCV. The observed sensitivity to GCV as seen with both devices in the presence of inducer is in line with studies overexpressing HSV-TK [19]. These results demonstrate that rewired endogenous signaling pathways can regulate apoptosis using either a suicide gene therapy system or overexpression of a proapoptotic gene.

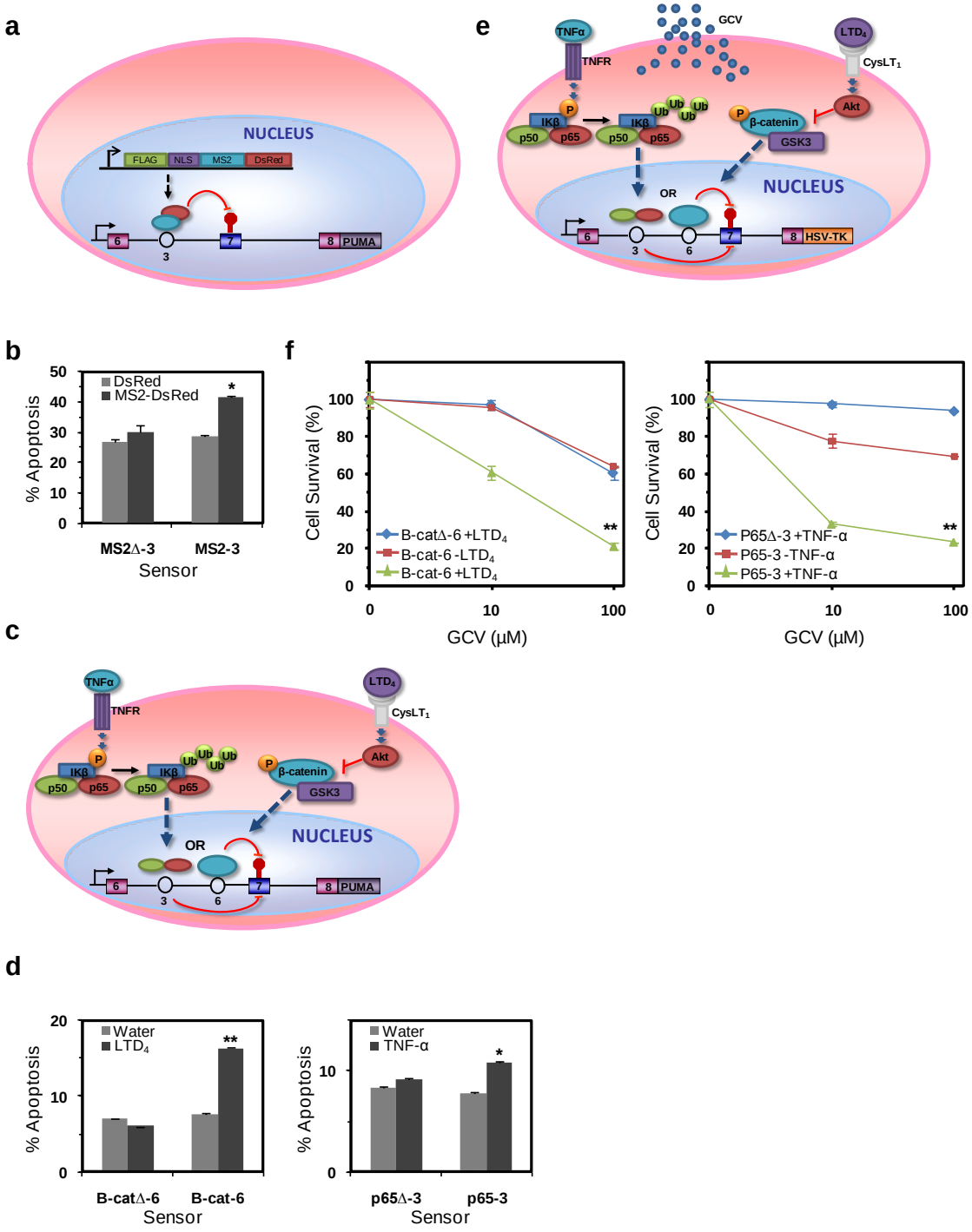

Figure 3.4. Platform mediated regulation of apoptosis. **(a)** MS2 splicing regulatory platform to induce apoptosis. The MS2 sensor component was inserted into position 3 of a framework consisting of Puma fused 3' of the SMN1 mini-gene. **(b)** Flow cytometry

analysis of apoptotic HEK-293 FLP-In stable cell containing the MS2 regulatory devices that mediate Puma induced apoptosis. Regulatory activity was assessed in the presence of the MS2-DsRed fusion and absence of the fusion (DsRed only) compared to mutant aptamer containing control constructs. **(c)** NF-κB p65 and β-catenin regulatory platforms to induce apoptosis. The NF-κB p65 and β-catenin sensor components were inserted into positions 3 and 6 of the framework respectively. The platform consists of Puma fused 3' of the SMN1 mini-gene. Cells were stimulated with either 20ng/ml TNF-α or 80 nM LTD_4 to induce the NF-κB or β-catenin pathways respectively. **(d)** Flow cytometry analysis of apoptotic HEK-293 FLP-In stable cell containing the NF-κB p65 and β-catenin regulatory devices that mediate Puma induced apoptosis. Regulatory activity was assessed in the presence of either inputs (TNF-α or LTD_4) and absence of both compared to mutant aptamer containing control constructs. **(e)** NF-κB p65 and β-catenin regulatory platforms to induce apoptosis using the HSV-TK suicide gene system. The NF-κB p65 and β-catenin sensor components were inserted into positions 3 and 6 of the framework respectively. The platform consists of HSV-TK fused 3' of the SMN1 mini-gene. Ganciclovir (GCV) was added to the cells to induce cell death. **(f)** Flow cytometry analysis of apoptotic HEK-293 FLP-In stable cell containing the NF-κB p65 and β-catenin regulatory devices that mediate HSV-TK induced cell death. Regulatory activity was assessed in the presence of either inputs (TNF-α or LTD_4) and absence of both compared to mutant aptamer containing control constructs.

3.3. Discussion

We have developed a novel framework for construction of both single and multiple input-single output RNA regulatory devices. We demonstrated that component modularity enabled the sensing of both heterologous as well as endogenous proteins and can be used to regulate the expression of any gene. Our platform can be interfaced with natural gene regulatory networks and signaling pathways to create programmable cells or cellular biosensors. The extension of our framework towards the processing of multiple inputs can be used in the creation of RNA-based platforms with sophisticated functionalities and to create complex gene regulatory networks to interrogate and program cellular function. Our platform can utilize both heterologous as well as reprogrammed endogenous signaling pathways to regulate apoptosis demonstrating the integration of cellular function to create complex user defined phenotypes. The platforms described here represent powerful tools to regulate gene expression and have broad applications in health and medicine where they can be used as 'intelligent' therapeutics towards the treatment and diagnosis of disease.

3.4. Materials and Methods

3.4.1. Base RNA device constructs

Plasmids were constructed using standard molecular biology techniques[20]. All enzymes, including restriction enzymes and ligases, were obtained through New England Biolabs unless otherwise noted. DNA synthesis was performed by Integrated DNA Technologies, Inc and DNA 2.0. Ligation products were electroporated into *E. coli* DH10B (Invitrogen) using a GenePulser XP system (BioRAD), and clones verified

through colony PCR and restriction mapping. All cloned constructs were sequence verified through Laragen. Primer sequences and plasmid descriptions are available in Tables S3.1 and S3.2, respectively.

The SMN1-GFP mini-gene fusion construct (pCS3001) was constructed through PCR amplification, digestion and ligation in the appropriate expression vector. A region encompassing the last nine nucleotides of exons 6 through the first 21 nucleotides of exon 8 of the *SMN1* mini-gene was amplified through PCR from template pCS3030 with primers Ex6 and Ex8 and PfuUltra II fusion high-fidelity DNA polymerase (Stratagene) and the resulting PCR product was digested with Nhe I. The *SMN1* mini-gene DNA synthesis was performed by DNA 2.0 to contain restriction sites Kpn I, Eco RV, Cla I (positions -87, -61 and -50 from 3'ss of exon7, respectively) and Xho I, Hind III, Bam HI, and Xba I (positions +10, +50, +70 and +97 from 5'ss of exon 7, respectively). The *GFP* gene was amplified from the template pKW430[21] with primers GFP1 and GFP2. The resulting PCR product was digested with Apa I and Nhe I and ligated into the corresponding restriction sites of the mammalian expression vector pcDNA5/FRT (Invitrogen). The SMN1-minigene PCR product was then ligated into the Nhe I restriction site of the resulting construct, creating the vector SMN1-GFP. The aptamer sequences used in this study are CGTACACCATCAGGGTACG[22], for MS2; CGTACCCATCAGGGTACG,[22] for MS2Δ; AGGCCGATCTATGGACGCTA AGGCACACCGGATACTTTAACGATTGGCT[23], for β-catenin; TCGGTTAGC AATTTCATAGGCCACACGGATATCGCAGGTATCTAGCCGGA (reverse compliment), for β-cateninΔ; GCATCCTGAAACTGTTTTAAGGTTGGCCGATGC[14], for NF-κB p50(1); CGTAGCCGGTTGGAAT TTTGTCAAAGTCCTACG (reverse

compliment), for NF-κB p50(1)Δ; GATCTTGAAACTGTTTTAAGGTTGGCCGATC[13], for NF-κB p50(2); GAAGCTTACAAGAAGGACAGCACGAATAAAACC TGCGTAAATCCGCCCCATTTGTGTAAGGGTAGTGGGTCGAATTCCGCTCA[12], for NF-κB p65; and ACTCGCCTTAAGCTGGGTGATGGGAATGTGT TTACCCCGCCTAAATGCGTCCAAAATAAGCACGACAGGAAGAACATTCGAAG (reverse compliment), for NF-κB p65Δ.

Specific aptamer and mutant cassette sequences containing portions of the SMN1-minigene were digested and ligated into the appropriate restriction sites within the SMN1-GFP construct (Table S3.3). Briefly, cassettes containing the wildtype and mutant MS2 coat protein aptamers were annealed, digested with the appropriate restriction enzymes and ligated into SMN1-GFP. β-catenin aptamer constructs were generated through PCR using templates β-cat-3, β-catΔ-3, β-cat-6, and β-catΔ-6 with forward primers Bcat3, BcatΔ3, Bcat6, and BcatΔ6 respectively with reverse primer AptRv. Similarly, for the NF-κB p50 and p65 aptamer constructs, the templates; NF-κBp50(1)-3, NF-κBp50(1)Δ-3, NF-κBp50(2)-3, NF-κBp65-3, and NF-κBp65Δ-3 were PCR amplified with forward primers p50(1), p50(1)Δ, p50(2), and p65, respectively, with reverse primer AptRv. The resulting β-catenin, NF-κB p50 and p65 PCR products were digested with the appropriate restriction enzymes and ligated into the corresponding restriction sites of SMN1-GFP. To construct RNA devices containing the wildtype and mutant MS2 coat protein aptamers in positions 3 and 10, the MS2-3 and MS2Δ-3 annealed cassettes were digested with Eco RV and Xho I and ligated into the corresponding restriction sites of SMN1-GFP containing the wildtype and mutant MS2 coat protein aptamers in position 10 (pCS3018 and pCS3019, respectively). To construct RNA devices containing the

wildtype and mutant NF-κB p65 aptamers in position 3 and the wildtype and mutant MS2 coat protein aptamers, the NF-κB p65 PCR products from above were digested with Eco RV and Xho I and were ligated into the corresponding restriction sites of SMN1-GFP containing the wildtype and mutant MS2 coat protein aptamers in position 10.

The SMN1-Puma and SMN1-TK fusions were constructed in two steps. The human *Puma* gene was amplified from template pORF5-hPUMA (Invivogen) with primers Puma1 and Puma2 to contain a flexible Gly-Ser linker (GGSGGS) at the 5' end. The resulting PCR product was digested with Nhe I and Pme I and ligated into the corresponding restriction sites of pcDNA5/FRT. The SMN1-GFP constructs containing the wildtype and mutant MS2 coat protein, β-catenin and NF-κB p65 aptamers in positions 3 and 6 of *SMN1* intron 6 (Figure 3.1a) were digested with Nhe I and the resulting SMN1-minigenes were ligated into the corresponding restriction site in the above vector containing the *Puma* gene. The resulting constructs are MS2-3-Puma, MS2Δ-3-Puma, β-cat-6-Puma, β-catΔ-6-Puma, p65-3-Puma and p65Δ-3-Puma (pCS3004-pCS3009, Table S3.2). Similarly, to create the SMN1-TK constructs the *HSV-TK* gene was amplified from the template CD19t-Tk-T2A-IL15op_epHIV7 using primers TK1 and TK2. The resulting PCR product was digested with Nhe I and Pme I and ligated into corresponding restriction sites of pcDNA5/FRT. The Nhe I digested SMN1-minigenes containing the wildtype and mutant β-catenin and NF-κB p65 aptamers in positions 3 and 6 of *SMN1* intron 6 were ligated into the corresponding restriction site of the above vector containing the *HSV-TK* gene. This created constructs β-cat-6-TK, β-catΔ-6-TK, p65-3-TK, and p65Δ-3-TK (pCS3010-–pCS3013, Table S3.2).

To create the MS2-DsRed control construct (pCS3014), the *DsRed* monomer gene was amplified from template pDsRed-monomer (Clontech) with primers DsRed1 and DsRed2, digested with Bam HI and Not I and ligated into the corresponding restriction sites of pcDNA5/FRT. The *MS2 coat protein* gene was amplified in two steps from template pHis-BIVT-MS2-RSp55[24] using primers MS2-1 and MS2-2 for the first round and MS2-3 and MS2-2 for the second to include a FLAG epitope (DYKDDDDK)[25] followed by an SV40 NLS (PKKKRKV)[26], 5' of the *MS2* gene. The final PCR product was digested with Kpn I and Bam HI and ligated into the corresponding restriction sites of the above vector containing DsRed monomer. The NF-κBp50-DsRed expression construct (pCS3015) was assembled similarly where the *NF-κB p50* gene was amplified in two steps from template pGAD424[27] using primers p50-1 and p50-2 for the first round and p50-3 and p50-2 to include a FLAG epitope followed by a SV40 NLS, 5' of the *NF-κB p50* gene. The final PCR product was digested with Nhe I and Kpn I and ligated into the corresponding restriction sites of the above vector containing DsRed monomer.

3.4.2. Cell culture, transfections, stable cell lines and flow cytometry

HEK-293 FLP-In cells (Invitrogen) were cultured in D-MEM supplemented with 10% fetal bovine serum (FBS) and 100 μg/ml Zeocin at 37ºC in 5% CO_2. Transfections were carried out with Fugene (Roche) according to the manufacturer's instructions. All cell culture media was obtained from Invitrogen.

HEK-293 FLP-In stable cell lines were generated by co-transfection of the appropriate SMN1 mini-gene construct with a plasmid encoding the Flp recombinase (pOG44) in growth medium without Zeocin according to the manufacturer's instructions (Invitrogen). Stable selections were carried out in 6-well plates seeded with ~$2x10^5$ HEK-293 FLP-In cells per well where 1.8 µg of pOG44 and .2 µg of the SMN1 mini-gene construct (10:1 ratio) were co-transfected. Fresh medium was added to the cells 24 h after transfection. The cells were expanded by a 1:4 dilution and Hygromycin B was added to a final concentration of 200 µg/ml 48 h after transfection. Clones were harvested by trypsinization, pooled and analyzed using a Quanta Cell Lab Cytometer (Beckman Coulter; Fullerton, CA) 10-14 days after transfection. GFP and DsRed fluorescence was excited at 488 nm and emission was measured through a 525-nm filter and a 610-nm band-pass filter respectively. For the NF-κB induction studies, cells were treated with 20ng/mL TNF-α (Sigma) for 48 h where indicated[28]. For the β-catenin induction studies, cells were serum starved 2h before stimulation with 80nM leukotriene D_4 (LTD_4) (Sigma) for 48 h in the absence of serum[29].

For transient transfection studies, HEK-293 stable cell lines containing SMN1 mini-genes were seeded in 24-well plates at ~$5x10^4$ cells per well 16 to 24 h prior to transfection. Cell lines were transfected with 250 ng of the appropriate MS2-DsRed or NF-κBp50-DsRed expression constructs. The cells were harvested by trypsinization, pooled and analyzed by flow cytometry 48 h after transfection. Experiments were carried out on different days and transfections were completed in duplicate, where the mean GFP fluorescence of the DsRed transfected population and the average error between samples is reported. For the induction of β-catenin and NF-κB pathways, HEK-293 stable cell

lines containing SMN1 mini-genes were seeded in a 24-well plate at ~$5x10^4$ cells per well 16 to 24 h prior to induction with LTD_4 or TNF-α. Stimulation of both pathways was carried out for 48h and the cells were harvested by trypsinization, pooled, and analyzed by flow cytometry. For the ganciclovir (GCV) sensitivity assays, HEK-293 stables cell lines containing SMN1 mini-genes containing either the β-catenin and NF-κB p65 aptamers were seeded in a 24-well plate at ~$5x10^4$ cells per well 16 to 24 h prior to induction with LTD_4 or TNF-α. At the time of induction cells were either left untreated or incubated with increasing concentrations of GCV (10 or 100μM). After 96h the cells were harvested by trypsinization, pooled, and analyzed by flow cytometry.

3.4.3. Apoptosis assays

Stable cell lines were harvested by trypsinization as described above. Pooled cells were washed in cold phosphate-buffered saline (PBS). Cells were stained with Pacific Blue annexin V and 7-aminoactinomycin D (7-AAD) using the Vybrant Apoptosis Assay Kit (Invitrogen) according to the manufacturer's instructions. The fluorescence of the stained cells was measured using a Quanta Cell Lab Cytometer where the Pacific Blue dye was excited using a UV light source and measured through a 465/430 band-pass filter (FL1). GFP and 7-AAD were excited with a 488-nm laser and measured through a 535-nm band-pass (FL2) and 670-nm long pass filter (FL3) respectively.

3.4.4. qRT-PCR analysis

Total cellular RNA was purified from stably transfected HEK-293 Flp-In cells using GenElute mammalian total RNA purification kit (Sigma) according to the manufacturer's instructions, followed by DNase treatment (Invitrogen). cDNA was synthesized using a gene-specific primer for the pcDNA5/FRT vector (SMN1cDNA) and Superscript III reverse transcriptase (Invitrogen) according to the manufacturer's instructions. qRT-PCR analysis was performed using isoform-specific primers (Table S3.4) where each reaction contained 1 µL template cDNA, 10 pmol of each primer and 1X iQ SYBR green supermix (BioRAD) to a final volume of 25 µL. Reactions were carried out using a iCycler iQ system (BioRAD) for 30 cycles (95ºC for 15 s, 72ºC for 30 s). The purity of the PCR products was determined by melt curve analysis. Data analysis was completed using the iCycler IQ system software v.3.1.7050 (BioRAD). Isoform-specific relative expression was calculated using the ΔCt (change in cycling threshold) method4. Expression levels of duplicate PCR samples were normalized to the levels of *HPRT* (Hypoxanthine-guanine phosphoribosyltransferase**)**. Fold expression data is reported as the mean expression for each sample divided by either the mean untreated expression value or the expression of the mutant aptamer cell line $\pm$ the average error.

3.4.5. Statistical analysis

Data are expressed as normalized or fold expression $\pm$ average error where applicable. Student's *t*-test and Anova analyses were performed using Microsoft Excel. $P < .05$ were taken to be significant.

Acknowledgments

We thank K. Hertel for providing the pHis-BIVT-MS2-RSp55 construct, M. Jensen for providing CD19t-Tk-T2A-IL15op_epHIV7 and L. J Maher for providing pGAD24.

References

1. Wang, E.T. *et al.* Alternative isoform regulation in human tissue transcriptomes. *Nature* **456,** 470–476 (2008).

2. Black, D.L. Mechanisms of alternative pre-messenger RNA splicing. *Annu Rev Biochem* **72,** 291–336 (2003).

3. Wang, G.S. & Cooper, T.A. Splicing in disease: disruption of the splicing code and the decoding machinery. *Nat Rev Genet* **8,** 749–761 (2007).

4. Blencowe, B.J. Alternative splicing: new insights from global analyses. *Cell* **126,** 37–47 (2006).

5. Suess, B. & Weigand, J.E. Engineered riboswitches: overview, problems and trends. *RNA biology* **5,** 24–29 (2008).

6. Vaish, N.K. *et al.* Monitoring post-translational modification of proteins with allosteric ribozymes. *Nat Biotechnol* **20,** 810–815 (2002).

7. Ray, P.S. *et al.* A stress-responsive RNA switch regulates VEGFA expression. *Nature* **457,** 915–919 (2009).

8. Win, M.N., Liang, J.C. & Smolke, C.D. Frameworks for programming biological function through RNA parts and devices. *Chem Biol* **16,** 298–310 (2009).

9. Liu, H.X., Cartegni, L., Zhang, M.Q. & Krainer, A.R. A mechanism for exon skipping caused by nonsense or missense mutations in BRCA1 and other genes. *Nat Genet* **27,** 55–58 (2001).

10. Schneider, D., Tuerk, C. & Gold, L. Selection of high affinity RNA ligands to the bacteriophage R17 coat protein. *J Mol Biol* **228,** 862–869 (1992).

11. Lee, H.K. *et al.* beta-catenin regulates multiple steps of RNA metabolism as revealed by the RNA aptamer in colon cancer cells. *Cancer Res* **67,** 9315–9321 (2007).

12. Wurster, S.E. & Maher, L.J., 3rd Selection and characterization of anti-NF-kappaB p65 RNA aptamers. *Rna* **14,** 1037–1047 (2008).

13. Mi, J. *et al.* H1 RNA polymerase III promoter-driven expression of an RNA aptamer leads to high-level inhibition of intracellular protein activity. *Nucleic Acids Res* **34,** 3577–3584 (2006).

14. Chan, R. *et al.* Co-expression of anti-NFkappaB RNA aptamers and siRNAs leads to maximal suppression of NFkappaB activity in mammalian cells. *Nucleic Acids Res* **34,** e36 (2006).

15. Hoffmann, A., Levchenko, A., Scott, M.L. & Baltimore, D. The IkappaB-NF-kappaB signaling module: temporal control and selective gene activation. *Science* **298,** 1241–1245 (2002).

16. Buskirk, A.R. & Liu, D.R. Creating small-molecule-dependent switches to modulate biological functions. *Chem Biol* **12,** 151–161 (2005).

17. Christofk, H.R. *et al.* The M2 splice isoform of pyruvate kinase is important for cancer metabolism and tumour growth. *Nature* **452,** 230–233 (2008).

18. Beltinger, C. *et al.* Herpes simplex virus thymidine kinase/ganciclovir-induced apoptosis involves ligand-independent death receptor aggregation and activation of caspases. *Proc Natl Acad Sci U S A* **96,** 8699–8704 (1999).

19. Song, Y., Kong, B., Ma, D., Qu, X. & Jiang, S. Procaspase-3 enhances the in vitro effect of cytosine deaminase-thymidine kinase disuicide gene therapy on human ovarian cancer. *Int J Gynecol Cancer* **16,** 156–164 (2006).

20. Sambrook, J. & Russell, D.W., *Molecular Cloning: a laboratory manual*, 3 ed. (Cold Spring Harbor Laboratory Press, Cold Spring Harbor, NY, 2001).

21. Stade, K., Ford, C.S., Guthrie, C. & Weis, K. Exportin 1 (Crm1p) is an essential nuclear export factor. *Cell* **90,** 1041–1050 (1997).

22. Villemaire, J., Dion, I., Elela, S.A. & Chabot, B. Reprogramming alternative pre-messenger RNA splicing through the use of protein-binding antisense oligonucleotides. *J Biol Chem* **278,** 50031–50039 (2003).

23. Lee, H.K., Choi, Y.S., Park, Y.A. & Jeong, S. Modulation of oncogenic transcription and alternative splicing by beta-catenin and an RNA aptamer in colon cancer cells. *Cancer Res* **66,** 10560–10566 (2006).

24. Graveley, B.R., Hertel, K.J. & Maniatis, T. A systematic analysis of the factors that determine the strength of pre-mRNA splicing enhancers. *Embo J* **17,** 6747–6756 (1998).

25. Chubet, R.G. & Brizzard, B.L. Vectors for expression and secretion of FLAG epitope-tagged proteins in mammalian cells. *Biotechniques* **20,** 136–141 (1996).

26. Kalderon, D., Roberts, B.L., Richardson, W.D. & Smith, A.E. A short amino acid sequence able to specify nuclear location. *Cell* **39,** 499-509 (1984).

27. Cassiday, L.A. & Maher, L.J., 3rd Yeast genetic selections to optimize RNA decoys for transcription factor NF-kappa B. *Proc Natl Acad Sci U S A* **100,** 3930–3935 (2003).

28. Hellweg, C.E., Arenz, A., Bogner, S., Schmitz, C. & Baumstark-Khan, C. Activation of nuclear factor kappa B by different agents: influence of culture conditions in a cell-based assay. *Ann N Y Acad Sci* **1091,** 191–204 (2006).

29. Mezhybovska, M., Wikstrom, K., Ohd, J.F. & Sjolander, A. The inflammatory mediator leukotriene D4 induces beta-catenin signaling and its association with antiapoptotic Bcl-2 in intestinal epithelial cells. *J Biol Chem* **281,** 6776–6784 (2006).

Supplementary Information

Table S3.1. Primer sequences

Name	**Primer sequence (5' to 3')**
Ex6	GCGCGCTAGCATGTATTATATGGTAAGTAAT CACTCAGC
Ex8	ATAGCTAGCGCTGCT ACCTGC CAGC
GFP1	GCGCGCTAGCGTG AGCAAGGGCGAG
GFP2	GCGCGGGCCCTTAGTACAGCTCGTCCATGCC
Puma1	ATAGTTTAAACGGTGGTTCT GGTGGTTCTGCCCGCGCACGCCAGGAG
Puma2	GCGC GTTTAAACTTA ATTGGGCTCCATCTCGGG
TK1	GCGCGCTAGCGTGACAGGGGGAATG GC
TK2	GCGCGTTTAAACTTAGTTAGCCTCCCCCATCTC
DsRed1	ATAGGATCCGACAACACCG AGGACGTCAT
DsRed2	ATAGCGGCCGCCTACTGGGAGCCGGAG
MS2-1	AGCCAAAAAAAAAACGCAAAGTGGCTTCTAACTTTACTCAGTTCGTTC
MS2-2	ATAGGATCCACCACCACCACCGTAGATGCCG
MS2-3	ATAGGTACCATGGATTACAAGGATGACGATGACAAGCCAAAAAAAA AACGCAAAGTG GCTTCTAACTTTAC
P50-1	AGCCAAAAAAAAAACGCAAAGTGGCAGAAGATGATCCATATTTGGGAAG
P50-2	ATAGGTACCGTCATCACTTTTGTCACAACCTTC
P50-3	ATAGCTAGCATGGATTACAAGGATGACGATGACAAGCCAAAAAAAA AACGCAAAGTGGCAGAAGATGATCC
SMN1cDNA	TAGAAGGCACAGTCGAGG
Bcat3	ATATGATACTAGCTATCAGGCCGA
Bcat3Δ	ATATGATATCTAGCTATCTCGGTTAG

Bcat6	ATA TATCGATGTCTATAT AGCTATTTTTTT TAA CTT
Bcat6Δ	ATATATCGATGTCTATAT AGCTATTTTTTT TAA CTT
AptRv	ATACTCGAGCAGACTTACTCCTTAATTTAAGGAATG
p50(1)	ATATGA TATCTA GCT ATCCGCGC
p50(1)Δ	ATATGA TATCTA GCT ATCCGTAGC C
p50(2)	ATATGA TATCTA GCT ATCCGCGC
p65	ATAT GATATCTAGCTATCGAAGC TACAAG AAGGACAGCAC

Table S3.2. Plasmid constructs used in this work

Name	Description
pCS3001	SM1-GFP. Contains the wild-type SMN1 mini-gene fused to the C-terminus of GFP.
pCS3002	SMN1-Puma. Contains the wild-type SMN1 mini-gene fused to the C-terminus of Puma.
pCS3003	SMN1-TK. Contains the wild-type SMN1 mini-gene fused to the C-terminus of HSV-TK.
pCS3004	MS2-3-Puma. Wildtype SMN1 mini-gene containing the MS2 aptamer in position 3 of intron 6 fused to the C-terminus of Puma.
pCS3005	MS2Δ-3-Puma. Wildtype SMN1 mini-gene containing the mutant MS2 aptamer in position 3 of intron 6 fused to the C-terminus of Puma.
pCS3006	β-cat-6-Puma. Wildtype SMN1 mini-gene containing the β-catenin aptamer in position 6 of intron 6 fused to the C-terminus of Puma.
pCS3007	β-catΔ-6-Puma. Wildtype SMN1 mini-gene containing the mutant β-catenin aptamer in position 6 of intron 6 fused to the C-terminus of Puma.
pCS3008	p65-3-Puma. Wildtype SMN1 mini-gene containing the NF-κB p65 aptamer in position 3 of intron 6 fused to the C-terminus of Puma.
pCS3009	p65Δ-3-Puma. Wildtype SMN1 mini-gene containing the mutant NF-κB p65 aptamer in position 3 of intron 6 fused to the C-terminus of Puma.
pCS3010	β-cat-6-TK. Wildtype SMN1 mini-gene containing the β-catenin aptamer in position 6 of intron 6 fused to the C-terminus of HSV-TK.
pCS3011	β-catΔ-6-TK. Wildtype SMN1 mini-gene containing the mutant β-catenin aptamer in position 6 of intron 6 fused to the C-terminus of HSV-TK.
pCS3012	p65-3-TK. Wildtype SMN1 mini-gene containing the NF-κB p65 aptamer in position 3 of intron 6 fused to the C-terminus of HSV-TK.
pCS3013	p65Δ-3-TK. Wildtype SMN1 mini-gene containing the mutant NF-κB p65 aptamer in position 3 of intron 6 fused to the C-terminus of HSV-TK.
pCS3014	MS2-DsRed. Contains the FLAG-NLS-MS2 gene fused to the C-terminus of DsRed.

pCS3015	NF-κBp50-DsRed. Contains the FLAG-NLS-NF-κBp50 gene fused to the C-terminus of DsRed.
pCS3016	MS2-10. Wildtype SMN1 mini-gene containing the MS2 aptamer in position 10 of intron 7 fused to the C-terminus of GFP.
pCS3017	MS2Δ-10. Wildtype SMN1 mini-gene containing the mutant MS2 aptamer in position 10 of intron 7 fused to the C-terminus of GFP.
pCS3018	MS2-3. Wildtype SMN1 mini-gene containing the MS2 aptamer in position 10 of intron 7 fused to the C-terminus of GFP.
pCS3019	MS2Δ-3. Wildtype SMN1 mini-gene containing the mutant MS2 aptamer in position 10 of intron 7 fused to the C-terminus of GFP.

Table S3.3. Aptamer cassette sequences used in the construction of the RNA devices. Aptamer sequences are italicized and nucleotides added for strengthening aptamer secondary structure are in Red.

Name	**Position**	**Restriction sites**	**Cassette (5'-3')**
MS2-1	1	Kpn I/Cla I	ATATGGTACCAACA*CGTACACCATCAGGGT ACG*TCCATATAAAGCTATAGATATCTAGCT ATCGATATAT
MS2Δ-1	1	Kpn I/Cla I	ATATGGTACCAACA*CGTACCCATCAGGGTA CG*TCCATAT AAAGCTATAGATATCTAGCTATCGAT ATAT
MS2-2	2	Kpn I/Cla I	ATATGGTACCAACATCCATATAAAGCTAT*C GTACACCA TCAGGGTACG*AGATATCTAGCTATCGATTA T
MS2Δ-2	2	Kpn I/Cla I	ATATGGTACCAACATCCATATAAAGCTAT*C GTACCCATCAGGGTACG*AGATATCTAGCTA TCGATTAT
MS2-3	3	Eco RV/Xho I	ATATGATATCTAGCTATC*CGTACACCATCAG GGTACG*GA TGTCTATATAGCTATTTTTTTTAACTTCCTT TATTTTCCT TACAGGGTTTCAGACAAAATCAAAAAGAA GGAAGGTGCTCACATTCCTTAAATTAAGG AGTAAGTCTGCTCGAGA TAT
MS2Δ-3	3	Eco RV/Xho I	ATATGATATCTAGCTATC*CGTACCCATCAG GGTACG*GATGTCTATATAGCTATTTTTTTTA ACTTCCTTTATTTTCCTTACAGGGTTTCAGA CAAAATCAAAAAGAAGGAAGGTGCTCACA TTCCTTAAATTAAGGAGTAAGTCTGCTCGA GATAT
MS2-4	4	Cla I/Xho I	ATATATCGATGTCTATATAGCT*CGTACACC ATCAGGTACG*ATTTTTTTTAACTTCCTTTAT

			TTTCCTTACAGGGTTTCAGACAAAATCAAA AAGAAGGAAGGTGCTCACATTCCTTAAAT TAAGGAGTAAGTCTGCTCGAGATAT
MS2Δ-4	4	Cla I/Xho I	ATATATCGATGTCTATATAGCT*CGTACCCAT CAGGGTACG*ATTTTTTTTAACTTCCTTTATT TTCCTTACAGGGTTTCAGACAAAATCAAAA AGAAGGAAGGTGCTCACATTCCTTAAATT AAGGAGTAAGTCTGCTCGAGATAT
MS2-5	5	Cla I/Xho I	ATATATCGATGTCTATATAGCTATTTTTTTT AACTTC*CGTACACCATCAGGGTACG*CTTTAT TTTCCTTACAGGGTTTCAGACAAAATCAAA AAGAAGGAAGGTGCTCACATTCCTTAAAT TAAGGAGTAAGTCTGCTCGAGATAT
MS2Δ-5	5	Cla I/Xho I	ATATATCGATGTCTATATAGCTATTTTTTTT AACTTC*CGTACCCATCAGGGTACG*CTTTATT TTCCTTACAGGGTTTCAGACAAAATCAAAA AGAAGGAAGGTGCTCACATTCCTTAAATT AAGGAGTAAGTCTGCTCGAG ATAT
MS2-6	6	Cla I/Xho I	ATATATCGATGTCTATATAGCTATTTTTTTT AACTTCCTTTATTTTCCTTAC*CGTACACCAT CAGGGTACG*AGGGTTTCAGACAAAATCAA AAAGAAGGAAGGTGCTCACATTCCTTAAA TTAAGGAGTAAGTCTGCTCGAGATAT
MS2Δ-6	6	Cla I/Xho I	ATATATCGATGTCTATATAGCTATTTTTTTT AACTTCCTTTATTTTCCTTAC*CGTACCCATC AGGGTACG*AGGGTTTCAGACAAAATCAAA AAGAAGGAAGGTGCTCACATTCCTTAAAT TAAGGAGTAAGTCTG CTCGAGATAT
MS2-7	7	Cla I/Xho I	ATATATCGATGTCTATATAGCTATTTTTTTT AACTTCCTTTATTTTCCTTACAGGGTTTCAG ACAAAATCAAAAAGAAGGAAGGTGCTCAC ATTCCTTAAATTAAGGAGTAAGTCTG*CGTA CACCATCAGGGTACG*CTCGAGATAT
MS2Δ-7	7	Cla I/Xho I	ATATATCGATGTCTATATAGCTATTTTTTTT AACTTCCTTTATTTTCCTTACAGGGTTTCAG ACAAAATCAAAAAGAAGGAAGGTGCTCAC

			ATTCCTTAAATTAAGGAGTAAGTCTG*CGTA CCCATCAGGGTACG*CTCGAGATAT
MS2-8	8	Xho I/HindIII	ATATCTCGAGCCAGCATTA*CGTACACCATC AGGGTACG*TGAAAGTGAATCTTACTTTTGT AAAAAAGCTTATAT
MS2Δ-8	8	Xho I/HindIII	ATATCTCGAGCCAGCATTA*CGTACCCATCA GGGTACG*TGAAAGTGAATCTTACTTTTGTA AAAAAGCTTATAT
MS2-9	9	Xho I/HindIII	ATATCTCGAGCCAGCATTATGAAAGTGAA TCTTA*CGTACACCATCAGGGTACG*CTTTTGT AAAAAAGCTTATAT
MS2Δ-9	9	Xho I/HindIII	ATATCTCGAGCCAGCATTATGAAAGTGAA TCTTA*CGTACCCATCAGGGTACG*CTTTTGTA AAAAAGCTTATAT
MS2-10	10	Xho I/Bam HI	ATATCTCGAGCCAGCATTATGAAAGTGAA TCTTACTTTTGTAAAAAAGC*CGTACACCATC AGGGTACG*TTCTTTATGGTTTGTGGGATCC ATAT
MS2Δ-10	10	Xho I/Bam HI	ATATCTCGAGCCAGCATTATGAAAGTGAA TCTTACTTTTGTAAAAAAGC*CGTACCCATCA GGGTACG*TTCTTTATGGTTTGTGGGATCCA TAT
MS2-11	11	HindIII/Bam HI	ATATAAGCTTCTTTATGGTTTGT*CGTACACC ATCAGGGTACG*GGGATCCATAT
MS2Δ-11	11	HindIII/Bam HI	ATATAAGCTTCTTTATGGTTTGT*CGTACCCA TCAGGGTACGG*GGGATCCATAT
MS2-12	12	Bam HI/Xba I	ATATGGATCCAAATGTTT*CGTACACCATCAG GGTACG*TTGAACAGTTAATCTAGAATAT
MS2Δ-12	12	Bam HI/Xba I	ATATGGATCCAAATGTTT*CGTACCCATCAG GGTACG*TTGAACAGTTAATCTAGAATAT
β-cat-3	3	Eco RV/Xho I	ATATGATATCTAGCTATC*AGGCCGATCTATG GACGCTATAGGCACACCGGATACTTTAACGAT TGGCT*GATGTCTATATAGCTATTTTTTTTAA

			CTTCCTTTATTTTCCTTACAGGGTTTCAGAC AAAATCAAAAAGAAGGAAGGTGCTCACAT TCCTTAAATTAAGGAGTAAGTCTGCTCGAG ATAT
β-catΔ-3	3	Eco RV/Xho I	ATATGATATCTAGCTATC*TCGGTTAGCAATT TCATAGGCCACACGGATATCGCAGGTATCTA GCCGGA*GATGTCTATATAGCTATTTTTTTT AACTTCCTTTATTTTCCTTACAGGGTTTCAG ACAAAATCAAAAAGAAGGAAGGTGCTCAC ATTCCTTAAATTAAGGAGTAAGTCTGCTCG AGATAT
β-cat-6	6	Cla I/Xho I	ATATATCGATGTCTATATAGCTATTTTTTTT AACTTCCTTTATTTTCCTTAC*AGGCCGATCT ATGGACGCTATAGGCACACCGGATACTTTAAC GATTGGCT*AGGGTTTCAGACAAAATCAAAA AGAAGGAAGGTGCTCACATTCCTTAAATT AAGG AGTAAGTCTG CTCGAG ATAT
β-catΔ-6	6	Cla I/Xho I	ATATATCGATGTCTATATAGCTATTTTTTTT AACTTCCTTTATTTTCCTTAC*TCGGTTAGCA ATTTCATAGGCCACACGGATATCGCAGGTATC TAGCCGGA*AGGGTTTCAGACAAAATCAAA AAGAAGGAAGGTGCTCACATTCCTTAAAT TAAGG AGTAAGTCTG CTCGAG ATAT
NF-κBp50(1)-3	3	Eco RV/Xho I	ATATGATATCTAGCTATC*GCATCCTGAAACT GTTTTAAGGTTGGCCGATGC*GATGTCTATAT AGCTATTTTTTTTAACTTCCTTTATTTTCCT TACAGGGTTTCAGACAAAATCAAAAAGAA GGAAGGTGCTCACATTCCTTAAATTAAGG AGTAAGTCTG CTCGAG ATAT
NF-κBp50(1)Δ-3	3	Eco RV/Xho I	ATATGATATCTAGCTATC*CGTAGCCGGTTG GAATTTTGTCAAAGTCCTACG*GATGTCTATA TAGCTATTTTTTTTAACTTCCTTTATTTTCC TTACAGGGTTTCAGACAAAATCAAAAAGA AGGAAGGTGCTCACATTCCTTAAATTAAG

			GAGTAAGTCTG CTCGAG ATAT
NF-κBp50(2)-3	3	Eco RV/Xho I	ATATGATATCTAGCTATCCGCGC*GATCTTG AAACTGTTTTAAGGTTGGCCGATC*GCGCGGA TGTCTATATAGCTATTTTTTTTAACTTCCTT TATTTTCCTTACAGGGTTTCAGACAAAATC AAAAAGAAGGAAGGTGCTCACATTCCTTA AATTAAGGAGTAAGTCTG CTCGAG ATAT
NF-κBp65-3	3	Eco RV/Xho I	*GAAGCTTACAAGAAGGACAGCACGAATAAAA CCTGCGTAAATCCGCCCCATTTGTGTAAGGG TAGTGGGTCGAATTCCGCTCA*GATGTCTATA TAGCTATTTTTTTTAACTTCCTTTATTTTCC TTACAGGGTTTCAGACAAAATCAAAAAGA AGGAAGGTGCTCACATTCCTTAAATTAAG G AGTAAG
NF-κBp65Δ-3	3	Eco RV/Xho I	*ACTCGCCTTAAGCTGGGTGATGGGAATGTGT TTACCCCGCCTAAATGCGTCCAAAATAAGCAC GACAGGAAGAACATTCGAAG*GATGTCTATAT AGCTATTTTTTTTAACTTCCTTTATTTTCCT TACAGGGTTTCAGACAAAATCAAAAAGAA GGAAGGTGCTCACATTCCTTAAATTAAGG AGTAAG

Table S3.4. Primer sequences for transcript isoform analysis through qRT-PCR

Name	**Forward Primer (5' - 3')**	**Reverse Primer (5' - 3')**	**Isoform**
Pair 1	GTATTATATGGAAATGCTGG	GAA GGTGGTCACGAGGG	Ex6/8 and GFP
Pair 2	TAAATTAAGGAGAAATGCT	GAA GGTGGTCACGAGGG	Ex7/8 and GFP
Pair 3	CAAAGATGGTCAAGGTCGCAAG	GGCGATGTCAATAGGACTCC	HPRT